

Aligning and flocking of ellipsoidal Quincke rollers by flipping

Kai-Xuan He(何凯旋), Qi-Ying Ni(倪琦英), Xiao-Yi Zhou(周晓怡), Wen-De Tian(田文得), Kang Chen(陈康), and Tian-Hui Zhang(张天辉)

Citation: Chin. Phys. B, 2025, 34 (**7**): 076401. DOI: 10.1088/1674-1056/adc669
http://cpb.iphy.ac.cn; http://iopscience.iop.org/cpb

What follows is a list of articles you may be interested in

Initial-state dependence of phase behaviors in a dense active system

Lu Chen(陈璐), Bokai Zhang(张博凯), and Z. C. Tu(涂展春)
Chin. Phys. B, 2023, 32 (**8**): 086401. DOI: 10.1088/1674-1056/acca09

Learning physical states of bulk crystalline materials from atomic trajectories in molecular dynamics simulation

Tian-Shou Liang(梁添寿), Peng-Peng Shi(时朋朋), San-Qing Su(苏三庆), and Zhi Zeng(曾志)
Chin. Phys. B, 2022, 31 (**12**): 126402. DOI: 10.1088/1674-1056/ac98a4

Solid-to-molecular-orientational-hexatic melting induced by local environment determined defect proliferations

Zhanglin Hou(侯章林), Jieli Wang(王杰利), Ying Zeng(曾颖), Zhiyuan Zhao(赵志远), Xing Huang(黄兴), Kun Zhao(赵坤), and Fangfu Ye(叶方富)
Chin. Phys. B, 2022, 31 (**12**): 126401. DOI: 10.1088/1674-1056/ac8ce1

Anomalous bond-length behaviors of solid halogens under pressure

Min Wu(吴旻), Ye-Feng Wu(吴烨峰), and Yi Ma(马毅)
Chin. Phys. B, 2021, 30 (**7**): 076401. DOI: 10.1088/1674-1056/abf4bd

Novel structures and mechanical properties of Zr_2N: *Ab initio* description under high pressures

Minru Wen(文敏儒), Xing Xie(谢兴), Zhixun Xie(谢植勋), Huafeng Dong(董华锋), Xin Zhang(张欣), Fugen Wu(吴福根), and Chong-Yu Wang(王崇愚)
Chin. Phys. B, 2021, 30 (**1**): 016403. DOI: 10.1088/1674-1056/abb220

Aligning and flocking of ellipsoidal Quincke rollers by flipping

Kai-Xuan He(何凯旋)[†], Qi-Ying Ni(倪琦英)[†], Xiao-Yi Zhou(周晓怡)[†], Wen-De Tian(田文得)[‡], Kang Chen(陈康)[§], and Tian-Hui Zhang(张天辉)[¶]

Center for Soft Condensed Matter Physics and Interdisciplinary Research and School of Physical Science and Technology, Soochow University, Suzhou 215006, *China*

(Received 15 March 2025; revised manuscript received 24 March 2025; accepted manuscript online 28 March 2025)

Active rods propelled along their long axis align their velocities and orientations simultaneously in collision. However, as the propulsion is perpendicular to the long axis, velocity alignment becomes dynamically difficult. Here, we show that ellipsoidal Quincke roller propelled along their short-axis (perpendicular to the long axis) can align their velocities by flipping and form flocking with nematic order. The flipping arises from the reversible transition between the static parallel spinless state and the spinning transversal state of ellipsoidal Quincke rollers. This is possible only near (above) the critical field where both the parallel spinless state and the spinning transversal spinning are metastable. The flipping-facilitated alignment offers an extra aligning mechanism for elongate active agents, and the resulting active liquid crystals serve a model system to explore the defect dynamics as the propulsion deviates from the local nematic orientation which has not been addressed yet.

Keywords: Quincke roller, flocking, aligning, flipping

PACS: 64.60.–i, 05.65.+b, 87.18.Gh, 82.70.Dd

DOI: 10.1088/1674-1056/adc669 **CSTR:** 32038.14.CPB.adc669

1. Introduction

Active matters are composed of self-propelled particles which continuously converse energy into mechanical work.[1,2] Active matters widely exist in biological systems which ranges from microscopic bacteria,[3,4] actin filaments,[5,6] cell[7] to macroscopic fish schools[8] and bird flocks.[9,10] Various collective motions, such as flocking,[11] activity waves,[12] and vortices[13] can emerge spontaneously in active matters. In collective motions, active units move with the same speed and direction of their neighbors.[14,15] To form collective motions, active units have to align their velocities in collision.[16,17] The aligning interactions generally arise from local interactions between active particles. For example, self-propelled rods moving along their long axis, such as bacteria,[18] actin filaments,[19] and microtubules,[20] align their velocities parallelly or antiparallelly (apolar or nematic alignment) because of volume excluded effect and inelastic nematic collision.[21,22] At the same time, the orientations of rods are aligned as well, giving rise to active liquid crystals with nematic order.[23] In this case, the alignments of velocities and orientations are coupled. Similar phenomena were observed in systems of artificial self-propelled rods including shaken cylindrical granular particles,[21,24] and chemically driven Janus rods.[25,26]

In dilute systems, self-propelled rods can form polar clusters,[27] polar bands,[28] traveling polar bands,[29] stationary nematic bands,[19] and standing waves.[30] In dense systems, the alignment of rods leads to large-scale liquid crystals with nematic symmetry. However, in liquid crystals of active rods, topological defects can spontaneously generate or annihilate such that long-range nematic order is destructed and active turbulences form.[31] Distinct from passive liquid crystals, topological defects in active liquid crystals are active: They move, annihilate and form continuously. The emergence of active liquid crystals is widely involved in various subcellular processes.[32] Topological defects as organization centers play a critical role in regeneration.[33] Therefore, the motion of topological defects in active liquid crystals is of fundamental importance in understanding the dynamics of cellular processes, and has been studied extensively.

Several theoretical models of topological defects in active liquid crystals have been established.[34] These models focus on systems where active rods are propelled along their long axis such that active forces are parallel to local orientational order.[35,36] In this case, the active stress is proportional to nematic tensor, and the comet-like defects are propelled in the direction of active forces.[34] It is of great interests theoretically to know how the collective behaviors of active rods

[†]These authors contributed equally to this work.
[‡]Corresponding author. E-mail: tianwende@suda.edu.cn
[§]Corresponding author. E-mail: kangchen@suda.edu.cn
[¶]Corresponding author. E-mail: zhangtianhui@suda.edu.ecn

© 2025 Chinese Physical Society and IOP Publishing Ltd. All rights, including for text and data mining, AI training, and similar technologies, are reserved.

and the defect dynamics will be modified if active rods are propelled along their short axis. Experimentally, however, it is a challenge to prepare active rods propelled transversally along the short axis. In this case, ellipsoidal Quincke rollers serves a model system where the active ellipsoids are propelled transversally along the short axis.[37] Nevertheless, the observations show that as the elongated rollers are propelled along the short axis, there motions are impeded once the velocities are aligned antiparallely. In passive systems, thermal diffusion is helpful in dissolving the antiparallel state. Nevertheless, the self-propelled ellipsoids are strong in persisting the direction of velocity, which enhances the resistance to the alignment of orientations. As a result, dynamic clusters form. In the dynamic clusters, orientations are disordered and the mobility of ellipsoidal rollers is significantly reduced due to the jammed motion.[37] It demonstrates that as the shape polarity and the force polarity of elongated particles are not parallel to each other, the alignments of velocity and orientation compete with each other.

In previous studies, the motion of elongated Quincke rollers is constrained in two dimensions.[37,38] In this study, we show that ellipsoidal Quincke roller can align their motion and form active liquid crystals by flipping. The flipping arises from a reversal transition between the static parallel state and the transversal spinning state of ellipsoidal Quincke rollers. The resulting active liquid crystals travel perpendicularly to the direction of nematic order. This is distinct from conventional active liquid crystals.

2. Materials and methods

2.1. Experimental setup

Polystyrene ellipsoidal particles of an aspect ratio 2.0 are dispersed in a 0.12-mol/L (AOT/hexadecane) solution. The suspension is sealed between two indium-tin-oxide–coated (ITO) glass slides. The distance between the two slides is around 110 ± 10 μm. Dynamical processes are observed with a Nikon microscope (10× objective) and recorded at a rate of 1000 FPS. The positioning and tracking accuracy of particles can reach 100 nm (0.1 pixels) using IDL codes, with an orientation tracking accuracy of 0.0114.[49]

2.2. Critical electric field

For spherical Quincke rollers, the critical electric field is defined as the magnitude of the external electric field at which the spherical Quincke rollers can stably rotate in the solution. By analogy with the definition of the critical electric field for spherical particles, the critical electric field for ellipsoidal Quincke rollers is defined as the magnitude of the external electric field at which the ellipsoidal Quincke rollers transition from a static parallel spinless state to a spinning transversal state In this study, the critical electric field for the ellipsoidal Quincke rollers is approximately 1.6 V/μm.

2.3. Velocity autocorrelation

The velocity autocorrelation is calculated with the velocities of particles by

$$C_v(\Delta t) = \sum_i \left\langle \frac{\boldsymbol{v}_i(t)\cdot\boldsymbol{v}_i(t+\Delta t)}{|\boldsymbol{v}_i(t)|\cdot|\boldsymbol{v}_i(t+\Delta t)|} \right\rangle_t .$$

The results are averaged over time t and all concerned particles i.

2.4. Velocity–velocity spatial correlation

The velocity–velocity spatial correlation is calculated with the velocities of particles by

$$C_v(\Delta r) = \sum_i \left\langle \frac{\boldsymbol{v}_i(r)\cdot\boldsymbol{v}_j(r+\Delta r)}{|\boldsymbol{v}_i(r)|\cdot|\boldsymbol{v}_j(r+\Delta r)|} \right\rangle .$$

The results are averaged over time t and all concerned particles i.

3. Results

Ellipsoidal particles are obtained by stretching polystyrene spheres as described in references.[39–41] The ellipsoidal particles are propelled by an external electric field to rotate (Quincke rotation) and move on the plane perpendicular to the electric field.[37] To activate Quincke rollers, the electric field has to be above a critical value.[11,42] Below the critical field, the ellipsoidal particles are electrically polarized and aligned with their long axis along the direction of electric field, giving rise to the static parallel spinless state (PSS, Fig. 1(a)).[11,37,43] Above the critical field, PSS becomes unstable with respect to the spinning transversal state (STS, Fig. 1(a)). In STS, the dipole moment along the short axis leads to the torque for the rotation around long axis while the dipole moment along the long axis leads to the torque to tilt the long axis. The rotation around a tilted long axis results in the rotation around the electric field, giving rise the chirality of ellipsoidal rollers. In the absence of sliding, there is no translational motion along the long axis. In this system, thermal Brownian motion is absent because of the high viscosity of solvent.

In principle, it is possible for the ellipsoidal Quincke rollers to form large-scale collective motions in which the long axis is aligned in the same direction while all rollers rotate and move in the same direction perpendicular to the long axis (Fig. 1(a), parallel alignment). In practice, however, two ellipsoidal Quincke rollers colliding with different directions

of velocity form overwhelmingly the antiparallel alignment (Fig. 1(a)) in which the motions of rollers are impeded by each other because of the volume excluded effect and the persistence of propulsion, giving rise to the jamming and the reduction of mobility. As a result, collision of multiple particles leads to the formation of dynamic clusters (Figs. 1(b) and 1(d), Movie 1 in the supporting information).

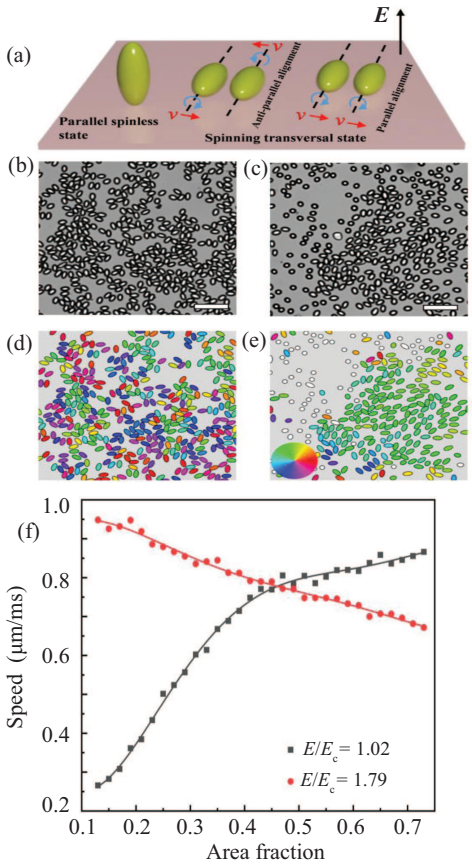


Fig. 1. Collective behavior of ellipsoidal Quincke rollers. (a) Below the critical electric field E_c, ellipsoidal Quincke rollers stay in the parallel spinless state with their long axis aligned with the electric field. Above E_c, ellipsoidal Quincke rollers roll on the plane perpendicular to the electric field. For two ellipsoidal rollers with the same orientation, their velocities can be parallel or antiparallel. In the antiparallel alignment, the persistent propulsion impedes the motion each other. (b) Dynamic clusters from at $E/E_c = 1.79$. The directions of velocities are presented by color in panel (d). (c) Flocking of ellipsoidal Quincke rollers observed at $E/E_c = 1.02$. The directions of velocities are colored in panel (e). (f) Dependence of speed on local density. The overall area fraction is $\phi = 0.4$, and the aspect ratio of ellipsoidal rollers is $k = 2.0$. Scale bar: 50 μm.

In dynamic clusters, it is dynamically blocked for rollers to reverse the direction of velocity by rotating the long axis in two-dimensional (2D) plane. In the absence of activity, the rollers can align their orientations spontaneously due to the volume excluded effect to reduce the free energy. For active ellipsoidal Quincke rollers, however, the electric dipolar interactions are significant and sensitive to local configurations. The dipolar interactions can stabilize various dynamic clusters rather than to align the long axis.[37] The dense clusters coexist with a dilute phase in which rollers move freely. This scenario is an analogue to the mobility-induced phase separation (MIPS) observed in active Brownian systems.[44,45] Nevertheless, the dense clusters of MIPS represent a stable dense phase while the dense clusters of ellipsoidal Quincke rollers are transient and have a finite life time.[37]

In our previous study observations were focused on where STS state is stable and the motion of ellipsoidal rollers is confined in two dimensions.[37] No flocking emerges therein. In this study, however, as E is near (above) the critical value E_c, flocking emerges unexpectedly as shown in Figs. 1(c) and 1(e) (Movie 2). At high electric field, the activity (speed) of ellipsoidal rollers is lower in dense clusters than that in low density regions because of the impeded motion (Fig. 1(f), $E = 1.79E_c$). However, accompanying the emergence of flocking, the dependence of activity (speed) on density is reversed: the higher the density, the higher the activity is. This is in consistent with the observations of spherical Quincke rollers.[46] The mechanism is that as Quincke rollers are aligned in velocity, the interaction between in-plane dipoles enhances the torque of Quincke rotation.[46] This mechanism is applicable to ellipsoidal Quincke rollers. To verify the emergence of flocking, the typical trajectories of ellipsoidal rollers observed under different electric field are followed (Fig. 2(a)). In consistent with the emergence of flocking, the trajectory near the critical field ($E = 1.12E_c$) is smooth and well-directed. Upon the increase of E, the trajectories become increasingly curved and irregular with random changes of direction. The mean squared displacements (MSD) at high electric field are characterized by two linear regions (Fig. 2(b)). At short time scale (< 10 ms), the mean square displacement $\langle \Delta r \rangle$ increases with time by t^2, suggesting a ballistic motion. At long time scale (> 100 ms), the MSD increases linearly with t. The ballistic behavior arises from the propelled motion between two sequential collisions with clusters. The rollers change their direction randomly each time as they collide with a cluster, giving rise to the long-time scale Brownian motion. As E approaches the critical value, the motion becomes persistent in direction because of the emergence of flocking. Velocity correlation functions offer an additional measurement about the persistence length and the persistence time of the motion. At high electric fields ($E = 1.79E_c$), the velocity autocorrelation decays down to 0.5 after 10 ms. Near the critical field ($E = 1.02E_c$), the strong correlation (> 0.5) persists up to 100 ms. The spatial velocity correlation (> 0.5) near the critical field extends up to 40 μm (Fig. 1(d), $E = 1.02E_c$) while at high electric field, only neighbored particles exhibit a weak correlation. Combining the above observations, it follows that collective motion emerges near the critical field.

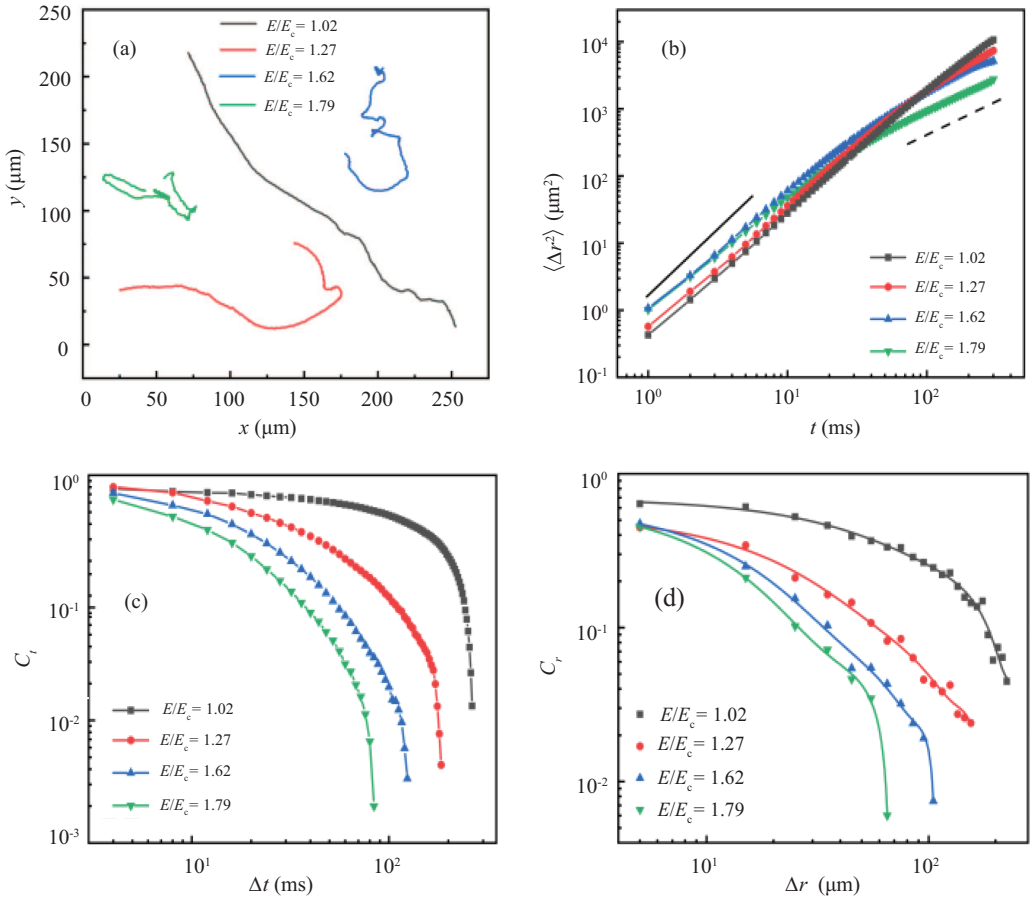


Fig. 2. Dynamic behavior of ellipsoidal Quincke rollers under different electric fields. (a) Typical trajectories of ellipsoidal Quincke rollers in 300 ms. (b) Means squared displacements (MSD). (c) Velocity autocorrelation. (d) Velocity–velocity spatial correlation.

To find out the mechanism underlying the emergence of flocking, the alignment of two ellipsoidal Quincke rollers at is followed (Movies 3(a)–3(d)). It is found that as two ellipsoidal rollers moving with different directions meet (Fig. 3(a)), they do not change their direction by 2D rotation. Instead, they stop rolling and flip to PSS by aligning their long axis along the direction of electric field (Figs. 3(b) and 3(e)).

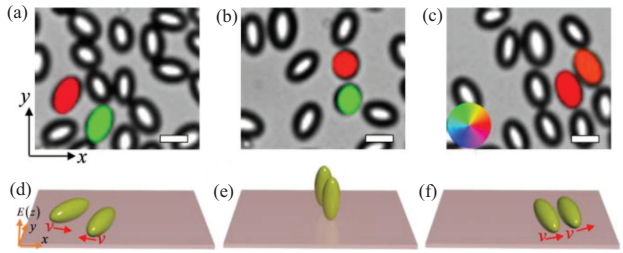


Fig. 3. Alignment of two rolling ellipsoidal Quincke rollers by flipping. (a) Spinning transversal state before colliding. (b) Parallel spinless state. (c) Aligned rolling. $E/E_c = 1.02$. Scale bar: 10 μm. (d)–(f) The three-dimensional (3D) schematics of the particle states in panels (a)–(c).

Nevertheless, the PSS of two rollers is not stable. They fall down and begin to roll with a common direction. The two ellipsoids align their velocities and orientations by flipping from STS to PSS. The aligning by flipping is observed at different colliding angles and different environment (Movies 3(b)–3(d)), representing a general mechanism near the critical field. The reversible transition between STS and PSS demonstrates that as E is above but close to the critical field, both STS and the PSS are metastable. The mechanism is that the stability of STS is dependent on the rotation speed around the long axis.

A high rotation speed can stabilize STS and suppress the flipping.[47] As the rotation speed decreases upon the decrease of E, the stability of STS decreases. Near (above) the critical field, isolated rollers can also transition reversibly between STS and PSS as shown in Fig. 4 (Movie 4) where the direction of rolling is selected randomly in the transition from PSS to STS. As two interacting spinless rollers fall down simultaneously, their rolling directions are coupled and aligned in the transition from PSS to STS as demonstrated in Fig. 3. Alternatively, if one static roller in PSS is collided by a moving roller, the transition from PSS to STS is not random in the selection of direction. Instead, the static roller falls down and starts to roll in the same direction of the impactor (Fig. 5, Movies 5(a) and 5(b)). It follows that near (above) the critical field, two ellipsoidal Quincke rollers in rolling states (STS and STS) or distinct states (STS and PSS) can align their velocities by flipping.

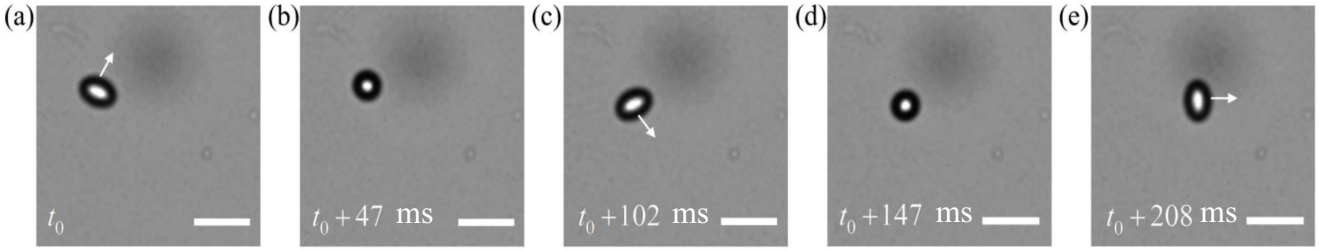


Fig. 4. Spontaneous flipping of individual ellipsoidal rollers. White arrows mark the direction of rolling. $E/E_c = 1.02$. Scale bar: 20 μm.

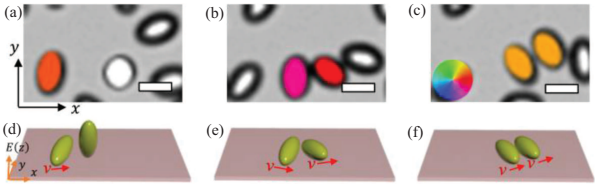


Fig. 5. A static spinless roller takes the same directions of the rolling roller after the collision. (a) The rolling particle is approaching the static spinless particle. (b) The spinless particle falls down with aligned orientation. (c) The two rollers are aligned both in velocity and orientation after the collision. $E/E_c = 1.02$. Scale bar: 10 μm. (d)–(f) The 3D schematics of the states in panels (a)–(c).

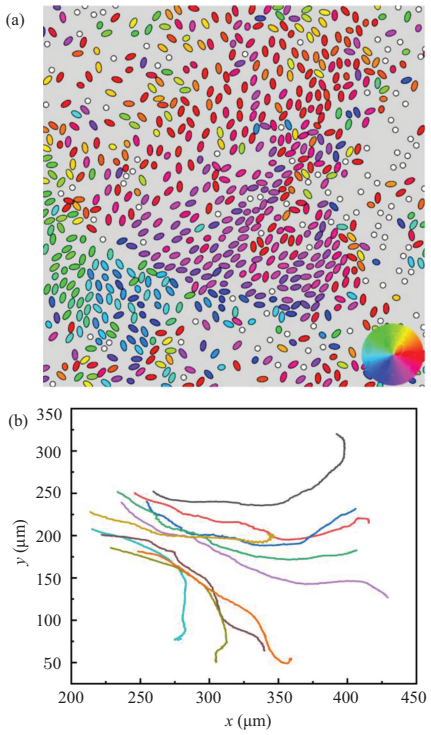


Fig. 6. Flocking of ellipsoidal Quincke rollers disassembles spontaneously due to the polydisperse chirality at $E/E_c = 1.02$. (a) Colored velocities in flocking. (b) Trajectories in flocking.

Above the critical field, the stability of STS is dependent on the mobility or the rotation angular speed around the long axis. Only as the angular speed is high enough, the long axis can be confined in the plane perpendicular to the field.[37] In general, however, the long axis is tilted with an acute angle to the plane. The tilted spinning leads to the rotation of long axis around the electric field, giving rise to the procession and curved trajectories. As a consequence, the motion of ellipsoidal Quincke rollers is characterized by a tunable chirality.[37] Increasing the electric field and the spinning angular speed can suppress the tilting. However, near (above) the critical field, the chirality of ellipsoidal Quincke rollers is remarkable such that motion is not persistent in direction. Quincke rollers with well-defined chirality can form steady vortices.[38] However, different from regular chiral particles, the chirality of ellipsoidal Quincke rollers is flexible in motion because the tilting of long axis is not steady in motion. Therefore, the chirality of ellipsoidal Quincke rollers in a flocking is polydisperse both in direction and curvature. As a result, the flocking of ellipsoidal Quincke rollers near the critical field is not stable (Fig. 6 and Movie 6): The flocking disassembles spontaneously because of the non-uniform chirality.

In summary, active rods propelled transversally are dynamically difficult to align their velocities in collision. Nevertheless, ellipsoidal Quincke rollers near (above) the critical field can align their velocities and form nematic order by flipping. The resulting active liquid crystals offer a model system for the exploring of defect dynamics in active liquid crystals in which active rods are propelled transversally. This is of great interests in extending and completing our understanding of active liquid crystals, considering the facts that existing theories and models are built on the observations of active rods driven along the axis. However, the nematic order of ellipsoidal Quincke rollers is not stable near the critical field because of the non-uniform chirality. In our recent studies,[48] it is found that ellipsoidal Quincke rollers driven by an alternating electric field can form steady large-scale collective motions with nematic order. In future studies, defect dynamics in the active liquid crystals of ellipsoidal Quincke rollers will be explored.

Acknowledgment

Tian-Hui Zhang acknowledges financial support of the National Natural Science Foundation of China (Grant No. 11974255).

References

[1] Das M, Schmidt C F and Murrell M 2020 *Soft Matter* **16** 7185
[2] Marchetti M C, Joanny J F, Ramaswamy S, Liverpool T B, Prost J, Rao M and Simha R A 2013 *Rev. Mod. Phys* **85** 1143
[3] Sokolov A, Aranson I S, Kessler J O and Goldstein R E 2007 *Phys. Rev. Lett.* **98** 158102
[4] Zhang H P, Be'er A, Florin E L and Swinney H L 2010 *Proc. Natl. Acad. Sci. USA* **107** 13626
[5] Butt T, Mufti T, Humayun A, Rosenthal P B, Khan S, Khan S and Molloy J E 2010 *J. Biol. Chem.* **285** 4964
[6] Schaller V, Weber C, Frey E and Bausch A R 2011 *Soft Matter* **7** 3213
[7] Deutsch A, Friedl P, Preziosi L and Theraulaz G 2020 *Philos. Trans. R. Soc. Lond B Biol. Sci.* **375** 20190377
[8] Katz Y, Tunstrom K, Ioannou C C, Huepe C and Couzin I D 2011 *Proc. Natl. Acad. Sci. USA* **108** 18720
[9] Cavagna A, Cimarelli A, Giardina I, Parisi G, Santagati R, Stefanini F and Viale M 2010 *Proc. Natl. Acad. Sci. USA* **107** 11865
[10] Ballerini M, Calbibbo N, Candeleir R, Cavagna A, Cisbani E, Giardina I, Lecomte V, Orlandi A, Parisi G, Procaccini A, Viale M and Zdravkovic V 2008 *Proc. Natl. Acad. Sci. USA* **105** 1232
[11] Bricard A, Caussin J B, Desreumaux N, Dauchot O and Bartolo D 2013 *Nature* **503** 95
[12] Liu Z T, Shi Y, Zhao Y F, Chaté H, Shi X Q and Zhang T H 2021 *Proc. Natl. Acad. Sci. USA* **118** e2104724118
[13] Bricard A, Caussin J B, Das D, Savoie C, Chikkadi V, Shitara K, Chepizhko O, Peruani F, Saintillan D and Bartolo D 2015 *Nat. Commun.* **6** 7470
[14] Vicsek T and Zafeiris A 2012 *Phys. Rep.* **517** 71
[15] Needleman D and Dogic Z 2017 *Nat. Rev. Mater.* **2** 17048
[16] Vicsek T, Czirók A, Ben-Jacob E, Cohen I and Shochet O 1995 *Phys. Rev. Lett.* **75** 1226
[17] Chaté H, Ginelli F, Grégoire G, Peruani F and Raynaud F 2008 *Eur. Phys. J. B* **64** 451
[18] Be'er A, Ilkanaiv B, Gross R, Kearns D B, Heidenreich S, Bär M and Ariel G 2020 *Commun. Phys.* **3** 66
[19] Huber L, Suzuki R, Krüger T, Frey E and Bausch A R 2018 *Science* **361** 255
[20] Sumino Y, Nagai K H, Shitaka Y, Tanaka D, Yoshikawa K, Chaté H and Oiwa K 2012 *Nature* **483** 448
[21] Kudrolli A, Lumay G, Volfson D and Tsimring L S 2008 *Phys. Rev. Lett.* **100** 058001
[22] Narayan V, Ramaswamy S and Menon N 2007 *Science* **317** 105
[23] Ginelli F, Peruani F, Bär M and Chaté H 2010 *Phys. Rev. Lett.* **104** 184502
[24] Blair D L, Neicu T and Kudrolli A 2003 *Phys. Rev. E* **67** 031303
[25] Paxton W F, Baker P T, Kline T R, Wang Y, Mallouk T E and Sen A 2006 *J. Am. Chem. Soc.* **128** 14881
[26] Wang W, Duan W, Sen A and Mallouk T E 2013 *Proc. Natl. Acad. Sci. USA* **110** 17744
[27] Zhang Z, Igoshin O A, Cotter C R and Shimkets L J 2018 *Biophys. J.* **115** 2499
[28] Be'er A, Strain S K, Hernández R A, Ben-Jacob E and Florin E L 2013 *J. Bacteriol.* **195** 2709
[29] Schaller V, Weber C, Semmrich C, Frey E and Bausch A R 2010 *Nature* **467** 73
[30] Börner U, Deutsch A, Reichenbach H and Bär M 2002 *Phys. Rev. Lett.* **89** 078101
[31] Dunkel J, Heidenreich S, Drescher K, Wensink H H, Bär M and Goldstein R E 2013 *Phys. Rev. Lett.* **110** 228102
[32] Doostmohammadi A and Ladoux B 2022 *Trends Cell Biol.* **32** 140
[33] Maroudas-Sacks Y, Garion L, Shani-Zerbib L, Livshits A, Braun E and Keren K 2021 *Nat. Phys.* **17** 251
[34] Doostmohammadi A, Ignés-Mullol J, Yeomans J M and Sagués F 2018 *Nat. Commun.* **9** 3246
[35] Genkin M M, Sokolov A, Lavrentovich O D and Aranson I S 2017 *Phys. Rev. X* **7** 011029
[36] Aranson I S 2019 *Phys. Usp.* **62** 892
[37] Chen Y, Wang L and Zhang T H 2023 *Soft Matter* **19** 512
[38] Zhang B, ASokolov A and Snezhko A 2020 *Nat. Commun.* **11** 4401
[39] Han Y, Alsayed A M, Nobili M, Zhang J, Lubensky T C and Yodh A G 2006 *Science* **314** 626
[40] Ho C C, Keller A, Odell J A and Ottewill R H 1993 *Colloid. Polym. Sci.* **271** 469
[41] Keville K M, Franses E I and Caruthers J M 1991 *J. Colloid Interface Sci.* **144** 103
[42] Jones T B 1984 *IEEE Trans. Ind. Appl.* **IA-20** 845
[43] Brosseau Q, Hickey G and Vlahovska P M 2017 *Phys. Rev. Fluids* **2** 014101
[44] Caporusso C B, Digregorio P, Levis D, Cugliandolo L F and Gonnella G 2020 *Phys. Rev. Lett.* **125** 178004
[45] Cates M E and Tailleur J 2015 *Annu. Rev. Condens. Matter Phys.* **6** 219
[46] Lu S Q, Zhang B Y, Zhang Z C, Shi Y and Zhang T H 2018 *Soft Matter* **14** 5092
[47] Cēbers A, Lemaire E and Lobry L 2000 *Phys. Rev. E* **63** 016301
[48] Unpublished results. The manuscript is in preparation. Movies are available
[49] Crocker J C and Grier D G 1996 *J. Colloid Interface Sci.* **179** 298